# Long-Term Controlled Protein Release from Poly(Ethylene Glycol) Hydrogels by Modulating Mesh Size and Degradation

Xinming Tong, Soah Lee, Layla Bararpour, Fan Yang*

Poly(ethylene glycol) (PEG)-based hydrogels are popular biomaterials for protein delivery to guide desirable cellular fates and tissue repair. However, long-term protein release from PEG-based hydrogels remains challenging. Here, we report a PEG-based hydrogel platform for long term protein release, which allows efficient loading of proteins via physical entrapment. Tuning hydrogel degradation led to increase in hydrogel mesh size and gradual release of protein over 60 days of with retained bioactivity. Importantly, this platform does not require the chemical modification of loaded proteins, and may serve as a versatile tool for long-term delivery of a wide range of proteins for drug-delivery and tissue-engineering applications.
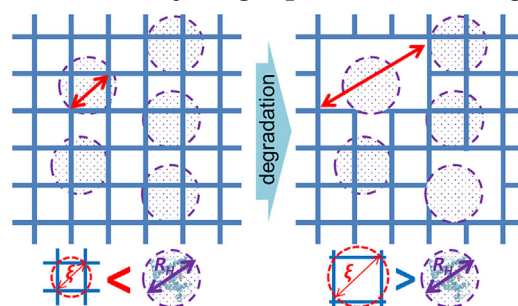
1. Introduction

Tissue development is guided by the orchestrated function of biological cues in a spatially and temporally controlled manner.[1] Thus, the controlled release of cues, such as protein cues, offers a powerful tool to aid tissue repair by promoting the processes that underlie desirable cellular fates.[2] The delivery of epidermal growth factor and transforming growth factor has been shown to accelerate wound healing.[3] Bone morphogenetic proteins have been widely used to promote bone regeneration,[4] while

X. Tong
Department of Orthopaedic Surgery, Stanford University, CA, 94305, USA
S. Lee
Department of Materials Science and Engineering, Stanford University, CA, 94305, USA
L. Bararpour
Department of Bioengineering, Stanford University, CA, 94305, USA
Prof. F. Yang
Departments of Orthopaedic Surgery and Bioengineering, Stanford University, CA, 94305, USA
E-mail: fanyang@stanford.edu

fibroblast growth factors and vascular endothelial growth factor (VEGF) potently accelerate angiogenesis.[5]

To deliver these biological signals in situ, previous studies have employed either systemic administration or oral delivery. However, these approaches generally result in low efficiency due to the large molecular size, poor absorption, and short half-life of growth factors.[2b] Biomaterials-based drug delivery platforms therefore hold great promise for enhancing tissue repair by recapitulating the soluble-factor environment that is present during normal tissue development. The activity of these proteins usually depends on their concentration, which necessitates their long-term and sustained release from the delivery material.[6] Of the various biomaterial-based platforms developed for protein delivery, hydrogels have been widely used due to their tissue-like water content, injectability, and tunability.[7] Polyethylene glycol (PEG) hydrogels are particularly attractive due to their biocompatibility[8] and biological inertness.[9]

Prolonged release from PEG-based hydrogels has been achieved via chemical conjugation of biomolecules to the hydrogel network through hydrolytically or enzymatically degradable linkages.[10] These chemical linkages may be designed with high specificity for biomolecules of interest[7c,10b] and trigger the release of these biomolecules in

response to stimuli such as matrix metalloproteinase.[10a] However, the high specificity of chemical conjugation, which is appropriate for small molecules, is more difficult to control when modifying large growth factors with complex structures. Proteins harbor many functional groups, which makes it hard, if not impossible, to specifically control the position and degree of conjugation.[11] Furthermore, chemical modification may lead to changes in protein structure[12] that may lower protein-receptor binding affinity and result in undesirable loss of biological activity.[13]

In contrast, physical entrapment inside the hydrogel network is a more facile method to incorporate proteins within hydrogel networks that does not require protein modification. Protein release is based only on passive diffusion through the hydrogel network.[8] The rate of protein release depends upon mesh size and upon the homogeneity of the hydrogel network. To achieve efficient protein loading and prolonged release, the mesh size of the network should be smaller than the hydrodynamic radius of the protein(s) of interest, but most current hydrogels have mesh sizes that are too large.[7b,14] Since PEG is bioinert and repulses proteins, entrapped proteins are likely to be released in bursts, with >80% of the cargo released within a few hours of encapsulation.[7b,14] Protein release is also sensitive to heterogeneity in the hydrogel network, which occurs when monomers crosslink in a random sequence. Linear PEG materials, such as PEG-diacrylate and PEG-dimethacrylate, are most commonly used for forming PEG hydrogels through a chain-growth radical polymerization. The intrinsic high dispersity of the polymerization degree from this radical polymerization typically yields heterogenous crosslinking density and network meshes, which result in poor control over protein release.[15,16] In contrast, step-growth polymerization involves crosslinking between end groups of multi-arm PEG molecules. Since the crosslinks are pre-defined as the cores of the multi-arm molecules, the hydrogel networks constructed through this method exhibit more defined structures, increased homogeneity, and increased control over mesh size.[14a,17]

The goal of the current investigation was to develop a step-growth polymerized, PEG-based hydrogel platform for sustained protein delivery via physical entrapment. It was hypothesized that with a mesh size smaller than the hydrodynamic radius of the growth factors, growth factors could be efficiently loaded into PEG hydrogels without burst release, and that the kinetics of protein release could be tuned by modulating hydrogel mesh size and degradation. To test this hypothesis, synthesized hydrogels with tunable mesh size were therefore synthesized by varying the PEG molecular weight between the crosslink and the PEG concentration (Figure 1). PEG hydrogel degradation was controlled with crosslinkers with three different degradation rates (Figure 1). Using bovine serum albumin (BSA) as a model protein, the effects of varying PEG mesh size and degradation on protein release over 2 months were examined. Finally, the release of basic fibroblastic growth factor (bFGF) from an optimized hydrogel formulation over 35 d was quantified. The ability of the released bFGF to stimulate cell proliferation was assessed using human adipose-derived stromal cells (hADSCs).

2. Results

2.1. Modulation of Hydrogel Mesh Size

To study the relationship between mesh size and hydrogel composition, the equilibrium swelling ratio on day 1 was used to calculate mesh size in the hydrogel. Mesh size
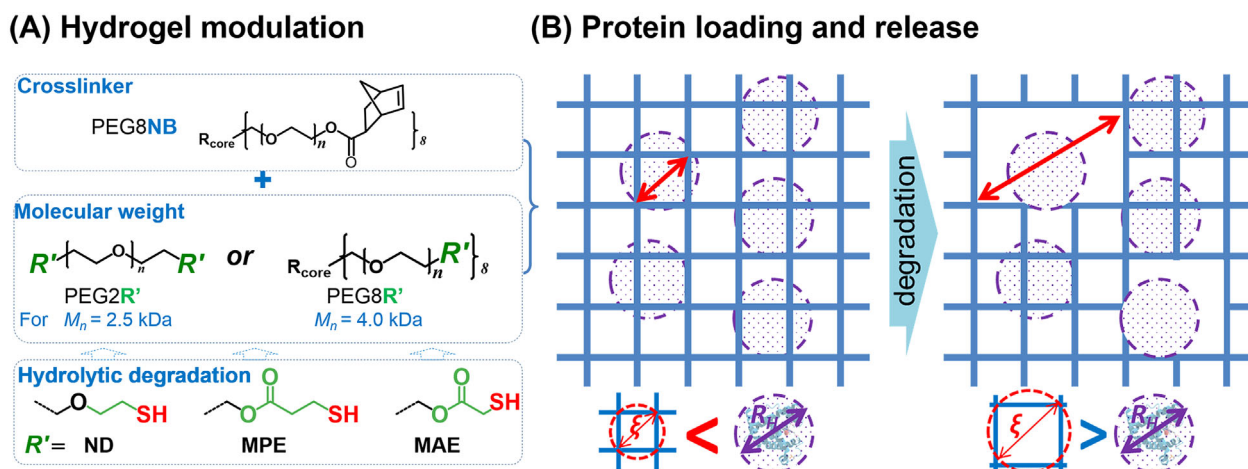

Figure 1. Strategy for controlling protein release from PEG hydrogels by tuning mesh size and degradation. (A) Chemical structures of PEG monomers with tunable molecular weight and hydrolytic degradation profiles. Terms and abbreviations are defined in section 2.2 and 2.3. (B) Physical entrapment of protein cargo in hydrogels with mesh size smaller than the hydrodynamic radius of the protein of proteins; release is triggered as hydrogels degrade.
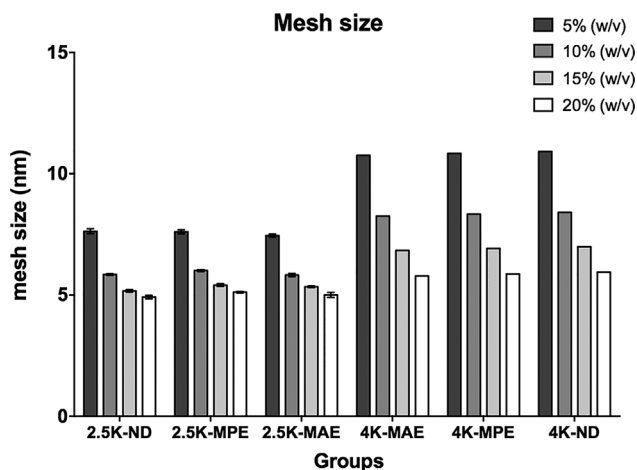
Long-Term Controlled Protein Release from Poly(Ethylene Glycol) Hydrogels. . .

Macromolecular
Bioscience

www.mbs-journal.de

Figure 2. Hydrogel mesh size depends on molecular weight (2.5 KDa vs. 4 KDa), degradable linkages (ND, MPE, MAE; see section 2.3 for a definition of the polymer naming convention) and PEG concentration (5% to 20%) (w/v). All hydrogels were swelled in PBS overnight to reach equilibrium. Mesh size was calculated using the equilibrium swelling ratio on day 1. Data are presented as mean ± standard deviation ($n = 4$).

increased when increasing the number average molecular weight between crosslinking points ($\overline{M}_n$), while the presence of degradable linkages did not alter mesh size (Figure 2). For example, increasing $\overline{M}_n$ from 2.5 kDa to 4.0 kDa in ND hydrogels increased mesh size from 4.92 ± 0.07 nm to 5.95 ± 0.01 nm ($p < 0.0001$), while the 2.5K-ND, 2.5K-MPE, and 2.5K-MAE hydrogels had comparable mesh sizes of 4.92 ± 0.07 nm, 5.12 ± 0.03 nm, and 5.01 ± 0.10 nm respectively ($p > 0.2$) (Figure 2). In addition, mesh size decreased with increasing PEG concentration for both 2.5 kDa and 4 kDa hydrogels.

2.2. Tunable Hydrogel Degradation

The effects on hydrogel degradation via varying the hydrolytic degradation of PEG crosslinks, molecular weight,

and PEG concentration were explored. Degradation was monitored by measuring the hydrogel swelling ratio over time. When $\overline{M}_n$ and PEG concentration were kept constant, hydrogels with MAE linkage showed the fastest degradation, both in hydrogels with $\overline{M}_n$ of 4K (Figure 3A) and 2.5K (Figure 3B). In contrast, the corresponding MPE and ND hydrogels maintained a stable swelling ratios up to 77 d (Figure 3A,B), indicating minimal degradation. Hydrogel degradation was also influenced by PEG molecular weight (Figure 3A,B). For example, 4K-MAE degraded in 24 d (Figure 3A), while 2.5K-MAE persisted for 74 d (Figure 3B). Changing the PEG concentration also influenced hydrogel degradation (Figure 3C). For the 2.5K-MAE hydrogel, increasing the PEG concentration from 5% to 20% slowed hydrogel degradation, with complete hydrogel degradation over 46 d and 74 d, respectively.

2.3. Controlled BSA Release

Cumulative protein release from PEG hydrogels with varying mesh size and degradation was then measured using BSA as a model protein. For non-degradable (ND) hydrogels, mesh size can be reduced by decreasing PEG $\overline{M}_n$ from 4K-ND to 2.5K-ND (Figure 2). A corresponding decrease in accumulative BSA release was observed from 2.5K-ND hydrogels (58%; Figure 4A) than in 4K-ND hydrogels (27%) by day 67 (Figure 4B). Incorporating a rapidly degradable linkage (MAE) into the hydrogels led to faster protein release, with >90% cumulative BSA release by day 67 from 2.5k-MAE hydrogels (Figure 4A,B). In contrast, incorporation of the degradable linkage MPE only mildly changed protein release compared to ND controls (Figure 4A,B). Lower PEG molecular weight and slower degradation led to delayed BSA release (Figure 4A,B), as did higher PEG concentrations (Figure 4C). For example, 5% (w/v) 2.5K-MAE hydrogels released ~74% protein in 24 h, but 7 d and 28 d were required to release the same amount of BSA from 10% (w/v) and 20% (w/v) hydrogels, respectively (Figure 4B,C).
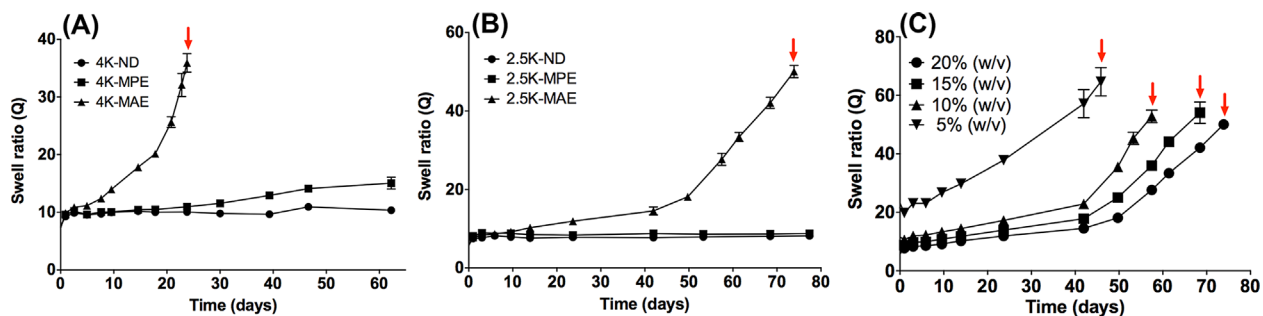

Figure 3. Hydrogel swelling over time depends on PEG molecular weight, degradable linkages, and concentration. Increased hydrogel degradation corresponds to increased hydrogel swelling ratio. (A) Swelling ratio of hydrogels (20% w/v) with $\overline{M}_n$ of 4 kDa. (B) Swelling ratio of hydrogels (20% w/v) with $\overline{M}_n$ of 2.5 kDa. (C) Swelling ratio of 2.5K-MAE hydrogels of varying PEG concentration. Data are presented as mean ± standard deviation ($n = 4$). Red arrows show time points after which the hydrogels were completely degraded.

Materials
Views

www.MaterialsViews.com

Macromol. Biosci. **2015,** *15,* 1679–1686
© 2015 WILEY-VCH Verlag GmbH & Co. KGaA, Weinheim
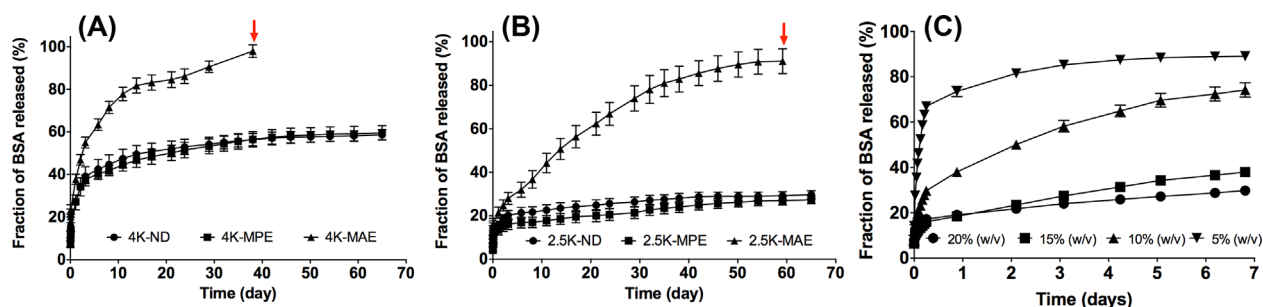
Macromolecular
Journals

1681

Figure 4. Tunable cumulative BSA release over time via varying PEG molecular weight, degradable linkages and concentration. (A) Profiles of BSA release from PEG hydrogels (20% w/v) with $\overline{M}_n$ of 4 kDa. (B) Profiles of BSA release from PEG hydrogels (20% w/v) with $\overline{M}_n$ of 2.5 kDa. (C) Profiles of BSA release hydrogels with varying PEG concentration and $\overline{M}_n$ of 2.5 kDa. Data are presented as mean ± standard deviation ($n = 4$). Red arrows show time points after which the hydrogels were completely degraded.
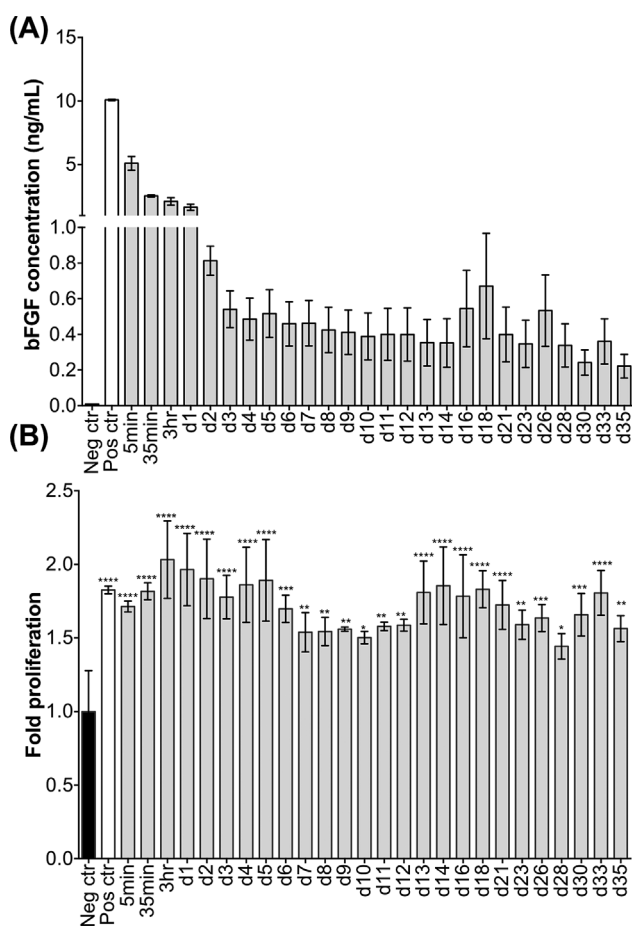

Figure 5. Sustained protein release over one month with retained biological activity. Release kinetics (A) and biological activity (B) of bFGF released from 2.5K-MAE hydrogels over one month. (A) Concentration bFGF released into supernatant over 35 d. (B) Biological activity of released bFGF was verified by quantifying its ability to stimulate cell proliferation of hADSCs. Data are presented as fold increase normalized to the proliferation of hADSCs cultured without bFGF (negative control (Neg ctr), black bar). $^*p < 0.05$, $^{**}p < 0.01$, $^{***}p < 0.001$, and $^{****}p < 0.0001$ relative to the negative control. Positive control (Pos ctr), freshly prepared 10 ng mL^{-1} bFGF. All data are presented as mean ± standard deviation ($n = 4$).

2.4. Sustained bFGF Release with Retained Functionality

To determine whether encapsulated proteins retain their biological activity throughout the processes of hydrogel formation, incubation, and degradation, bFGF was loaded into 2.5K-MAE hydrogels, and released protein was collected over time. Similar to the trends for BSA release (Figure 4), enzyme-linked immunosorbance assay indicated sustained bFGF release over 35 d (Figure 5A). The biofunctionality of released protein was also determined by adding released bFGF to hADSCs and measuring the resulting cell proliferation. bFGF released from 2.5K-MAE hydrogels stimulated hADSCs proliferation at 144–203%, which is comparable to the level of freshly prepared bFGF (10 ng mL^{-1}) (Figure 5B). Taken together, these results confirm that 2.5K-MAE hydrogels enable the sustained release of biologically active bFGF over 35 d.

3. Discussion

Here, a facile approach to control protein release from PEG hydrogels by modulating mesh size and degradation is demonstrated (Figure 1). Hydrogels with small mesh size were obtained via thiol-ene step growth polymerization. Changing hydrogel concentration and molecular weight are convenient handles for tuning mesh size. However, previous studies often considered the relationship between hydrogel mesh size and theoretical protein diffusivity but neglected the hydrodynamic radius of the protein cargo, which was often smaller than the hydrogel mesh.[7a,7b] Previous studies using hydrogels with mesh sizes above the size of BSA ($\sim$14×4×4 nm)[18] resulted in a burst (>60%) release of BSA release within an hour, and the remaining protein escaped the hydrogels in a few days.[7b] These results highlight the need for hydrogels with smaller mesh to allow more gradual protein release. In the present investigation, hydrogel mesh size was decreased to 4.92 nm, comparable to the size of BSA, by increasing the

www.MaterialsViews.com

Long-Term Controlled Protein Release from Poly(Ethylene Glycol) Hydrogels...

Macromolecular
Bioscience

www.mbs-journal.de

hydrogel concentration to 20% (w/v) and decreasing $\overline{M}_n$ to 2.5 kDa (Figure 2). As a result, BSA was physically entrapped in the hydrogel, with only 30% release after 67 d (Figure 4B). In contrast, hydrogels with larger mesh (5.95 nm) obtained from hydrogels with $\overline{M}_n$ of 4.0 kDa displayed lower protein retention (58% release) (Figure 4A). Hydrogels with smaller mesh retained BSA for up to 2 months. It was noted that BSA was not completely caged in hydrogels even with an average mesh size smaller that the radius of BSA. This was because although a step-growth polymerization was utilized to increase the homogeneity, there will still be some unavoidable defects due to the possible incomplete reaction of the functional groups and self-loop formation,[19] as well as the dispersity of the molecular weight distribution of PEG macromers.

To release the entrapped protein, hydrogels need to be degraded over time and thus enlarge the mesh size for controlled protein release. Hydrogel degradation triggered by hydrolysis or enzymes has been previously employed to promote protein release.[7b,14a,20] However, the initial mesh sizes of the hydrogels are often larger than loaded proteins, which lead to burst release even without degradation.[7b] Our hydrogels were designed to have an initial mesh size smaller than loaded proteins, and incorporated various degradable structures to allow tunable protein release (Figure 1A). The degradation rate of an ester linkage can be tuned by changing the number of methylene residuals between an ester and a thiol ether.[21] Therefore, it was expected that MPE linkages containing two methylene residuals between an ester and a thiol ether will yield an intermediate degradation rate, while MAE linkages, which contain only one methylene, would degrade more rapidly. Our results show that MPE hydrogels displayed a stable swell ratio that was similar to those calculated for hydrogels with non-degradable linkages (Figure 3A,B); this effect may due to the hydrophobicity of norbornene, which slows ester hydrolysis.[21a] MAE hydrogels degraded efficiently, as indicated by the increase of swell ratio over time (Figure 3), and 4K-MAE hydrogels (Figure 3A) underwent a more rapid increase in swell ratio than 2.5K-MAE hydrogels (Figure 3B), indicating faster degradation. Accordingly, faster degradation was accompanied by faster BSA release; 4K-MAE hydrogels released BSA in 38 d (Figure 4A), while 2.5K-MAE hydrogels needed 59 d (Figure 4B). These results suggest that more ester linkages between crosslink points (two in 4K-MAE hydrogels and one in 2.5K-MAE hydrogels) may also accelerate degradation and protein release. In addition, hydrogels with lower initial PEG concentrations degraded more rapidly (Figure 3C), and released protein faster (Figure 4C). It should be noted that although ester is good for introducing hydrolytic degradation for protein release, the control over degradation rate is still limited as shown in this study. To achieve a broader range of degradation and protein release,

alternative degradable structures may be introduced, such as carbamate, with a hydrolysis half-life that could be modulated from hours to months.[7c,10c]

Hydrogels with degradable linkages released their cargo when the protein passed through the enlarged mesh created by degradation (Figure 1B). MAE-containing hydrogels released >90% of the loaded BSA (Figure 4), indicating high efficiency of protein release. Previous studies have used the total amount of released protein rather than the initial loaded protein amount to calculate the release percentage.[22] This may lead to an overestimate of the efficiency of protein release by not taking into account the unreleased proteins. Faster degradation was accompanied by faster BSA release; 4K-MAE hydrogels released BSA in 38 d (Figure 4A), while 2.5K-MAE hydrogels needed 59 d (Figure 4B). Thus, although hydrogel degradation has been widely used to control protein release,[7b,14a] mesh size should be considered when tuning degradation. For example, decreasing the initial PEG concentration to accelerate degradation also resulted in a larger mesh size (Figure 2), which led to fast protein release (Figure 4C). Decreasing the concentration of 2.5K-MAE hydrogel to 5% (w/v), which showed a degradation period of 46 d, caused the release of 70% of the loaded BSA within 24 h due to the large initial mesh size (7.63 nm). But with a concentration of 10% (w/v), which leads to a decreased mesh size (5.85 nm), 2.5K-MAE hydrogel could then release 75% of the BSA over 7 d. Thus, to achieve sustainable long-term release, an appropriate initial mesh size and degradation rate are both essential.

To achieve prolonged protein release from hydrogels, molecules that possess protein-binding affinity, such as heparin or short peptides with specific binding affinity for the target proteins, have been incorporated.[23] However, such strategies only apply to proteins for which specific binding structures are available. In contrast, our method relies only on physical entrapment and no specific interactions are required for protein loading/release as the entrapment and release of loaded cargo is solely controlled by hydrogel mesh size and degradation. Thus, our method is more versatile and can be applicable for controlling the release of a broad range of proteins.

Here, thiol-ene addition chemistry was chosen for hydrogel crosslinking due to its high efficiency and homogeneity.[24] This crosslinking mechanism was also chosen because previous studies have used it for protein encapsulation in hydrogels, and it showed minimum interference with protein bioactivity.[14a,25] Similarly, it is demonstrated here that bFGF encapsulated in our hydrogels retained its biofunctionality after release (Figure 5B). Although a relatively high amount of bFGF was released in the first few hours, possibly because the hydrodynamic radius of bFGF is smaller (∼3–4 nm)[26] than that of BSA, sustained release was observed over the following month

Materials
Views
www.MaterialsViews.com

Macromol. Biosci. **2015,** *15,* 1679–1686
© 2015 WILEY-VCH Verlag GmbH & Co. KGaA, Weinheim

Macromolecular
Journals

1683

(Figure 5A). In contrast to strategies for protein delivery that require chemical conjugation[10b] or the incorporation of affinity structures to increase specificity,[27] our approach only required physical entrapment of proteins of interest in PEG hydrogels (Figure 1), and thus our strategy is likely to be appropriate for a broad range of biomedical applications. Chemical conjugation strategies need to be designed specifically for different biomolecules given the available modifiable functional groups, and may easily induce loss of bioactivity.[12,13] Our strategy can circumvent these limitations as the entrapment and release of loaded cargo is solely controlled by hydrogel mesh size and degradation. Although only employed photo-initiated thiol-ene addition was employed in the present study, other methods, including redox-initiated radical addition[28] and Michael addition,[7b] may expand the utility of our approach. It is also important to consider that some proteins of interests may possess free thiol groups that can interfere with the thiol chemistry based crosslinking, thus other crosslinking methods may be used, such as Diels-Alder coupling.[10b] Furthermore, other degradation strategies rather than hydrolysis, such as photodegradation[29] and enzymatic degradation,[14a] may also be employed to induce changes in hydrogel mesh size. The concept of achieving sustained protein release via controlling hydrogel mesh size and degradability may be broadly applicable using other polymers and hydrogels.

4. Conclusion

An approach for controlling protein release from PEG hydrogels by controlling mesh size and degradation has been demonstrated. By developing hydrogels with controllable mesh size through step growth polymerization, protein could be physically entrapped in hydrogel with small meshes. Tunable degradation was introduced by incorporating various degradable structures, thus yielding sustained protein release over one month with retained bioactivity. Since this approach only employed the physical processes of entrapment and degradation, it could be a very versatile method for delivering a broad range of proteins for diverse biomedical applications.

5. Experimental Section

5.1. Materials

Eight-arm PEG (MW $\sim$10 kDa) was purchased from JenKem Technology USA. Linear PEG-diol (MW $\sim$1.5 kDa), p-toluenesulfonic acid, mercaptoacetic acid, and 3-mercaptopropionic acid were purchased from Sigma-Aldrich USA. Lithium phenyl-2,4,6-trimethylbenzoylphosphinate (LAP) was synthesized as previously reported.[30] All other reagents and solvents were obtained from Fisher Scientific unless otherwise noted.

5.2. Synthesis of PEG Monomers

Eight-arm PEG-norbornene (PEG8NB), 8-arm PEG-thiol (PEG8SH), and linear PEG-dithiol (PEG2SH) were synthesized as previously reported.[24,31] Eight-arm PEG mercaptopropionic ester (PEG8MPE) was synthesized by reacting 8-arm PEG with mercaptopropionic acid in toluene. Briefly, 5.0 g of eight-arm PEG were dissolved in 150 mL of toluene, followed by the addition of 34 mg of p-toluenesulfonic acid. After adding 1.74 mL of 3-mercaptopropionic acid, the solution was refluxed overnight. The azeotropic mixture was collected periodically. After cooling the solution to room temperature, the product was precipitated in ice-cold diethyl ether. Eight-arm PEG mercaptoacetic ester (PEG8MAE) was synthesized by reacting 8-arm PEG with mercaptoacetic acid following the same procedure as for PEG8MPE. Linear PEG mercaptopropionic ester (PEG2MPE) and linear PEG mercaptoacetic ester (PEG2MAE) were synthesized via the protocols used for PEG8MPE and PEG8MAE.

5.3. Preparation of Hydrogels

To examine the effects of PEG mesh size and degradability on protein release, six PEG polymers were synthesized (Table 1). Specifically, PEG hydrogels with 2.5 kDa and 4.0 kDa average molecular weight between crosslinking points ($\overline{M}_n$) were

Table 1. Summary of hydrogel monomers and characteristics. Terms and abbreviations are defined in section 2.2 and 2.3.

Group	$\overline{M}_n$ [kDa]	PEG monomers (molar ratio)	Number of ester groups between crosslinks	Number of methylene groups between thiol ether and ester	Expected degradation
2.5K-ND	2.5	PEG8NB / PEG8SH (1:1)	0	0	None
2.5K-MPE	2.5	PEG8NB / PEG8MPE (1:1)	1	2	Intermediate
2.5K-MAE	2.5	PEG8NB / PEG8MAE (1:1)	1	1	Fast
4K-ND	4.0	PEG8NB / PEG2SH (5:3)	0	0	None
4K-MPE	4.0	PEG8NB / PEG2MPE (5:3)	2	2	Intermediate
4K-MAE	4.0	PEG8NB / PEG2MAE (5:3)	2	1	Fast

Long-Term Controlled Protein Release from Poly(Ethylene Glycol) Hydrogels...

Macromolecular
Bioscience

www.mbs-journal.de

synthesized. For each PEG $\overline{M}_n$, PEG degradability was further varied with three degradable linkages: a non-degradable linkage (ND), mercaptopropionic ester (MPE), and mercaptoacetic ester (MAE) (Table 1). All PEG monomers were dissolved in phosphate-buffered saline (PBS) with 0.05% (w/v) LAP at a concentration of 20% (w/v) before use. To make PEG hydrogels with 4.0 kDa $\overline{M}_n$ and ND linkages (4K-ND; this naming strategy was used to designate the other five PEG polymers) PEG8NB solution was mixed with PEG2SH at a volume ratio of 5:3 and exposed to ultraviolet light at 4 mW cm^{-2} for 5 min. Other hydrogels were fabricated following similar procedures. To make lower-concentration hydrogels (15% (w/v), 10% (w/v), and 5% (w/v)), a 20% (w/v) monomer solution was further diluted in PBS (with 0.05% (w/v) LAP) and crosslinked under ultraviolet light.

5.4. Calibration of PEG Concentration

All hydrogels were prepared in a cylindrical mold using a volume of 50 µL per sample. Wet weight was measured directly after hydrogel formation. All hydrogels were incubated in deionized water overnight at room temperature to remove unreacted PEG monomers, then lyophilized. Dry weight was then measured and divided by the wet weight to determine the calibrated PEG hydrogel concentration.

5.5. Swelling Ratio

Hydrogels were prepared (50 µL each) and incubated in a 48-well plate filled with 500 µL PBS per well at room temperature. Wet weight was measured at a predetermined time. The swelling ratio (Q) of hydrogels was calculated using Equation 1:

$$Q = \frac{W_{wet}/\rho_{gel}}{W_{dry}/\rho_{PEG}} \tag{1}$$

where W_{wet} is the wet weight of the hydrogel at each time point, W_{dry} is the dry weight of the hydrogel calculated by multiplying the hydrogel wet weight by the calibrated PEG concentration, and ρ_{PEG} and ρ_{gel} are the density of PEG and the hydrogel, respectively, which were defined as 1.12 g cm^{-3} and 1.01 g cm^{-3}, respectively, according to the literature.[32]

5.6. Calculation of Mesh Size

To reach equilibrium for swelling, hydrogels were incubated in PBS overnight after preparation. Mesh size (ξ) was calculated using Equation 2, in accordance with ref.:[33]

$$\xi = \upsilon_2^{-1/3}(\overline{r_0^2})^{1/2} \tag{2}$$

where υ_2 is the volume fraction of polymers in the hydrogels that have reached equilibrium in swelling (equal to the reciprocal of Q) and $(\overline{r_0^2})^{1/2}$ is the root-mean-squared end-to-end distance of the polymer chain in the unperturbed state, which can be calculated using Equation 3, in accordance with ref.:[34]

$$(\overline{r_0^2})^{1/2} = lC_\infty^{1/2}n^{1/2} \tag{3}$$

where l is the average bond length, C_n is the characteristic ratio of the polymer ($l = 0.154$ nm, $C_\infty^{1/2} = 4.0$[34]), and n is the number of

bonds in the chain, calculated as $3M_c/M_r$, where $\overline{M_c}$ was calculated from the Flory-Rehner equation (Equation 4) and M_r is the molecular weight of the repeating unit, which is 44 for PEG.

$$\frac{1}{\overline{M_c}} = \frac{2}{\overline{M_c}} - \frac{\frac{\overline{\upsilon}}{V_1}(\ln(1-\upsilon_2)+\upsilon_2+\chi_1\upsilon_2^2)}{\upsilon_2^{1/3}-\upsilon_2/2} \tag{4}$$

In Equation 4, $\overline{\upsilon}$ is the specific volume of the polymer (ρ_s/ρ_p), V_1 is the molar volume of the solvent (18 cm^3 mol^{-1} for water), χ_1 is the polymer-solvent interaction parameter (0.426 for PEG-water),[34] and υ_2 is the polymer volume fraction in the equilibrium swollen hydrogel (the reciprocal of the swell ratio).

5.7. Quantifying Protein Release

BSA was used as a model protein to characterize the profile of release from the PEG hydrogels. BSA was dissolved in PBS (with 0.05% (w/v) LAP) at concentration of 20 mg mL^{-1}. PEG monomers were dissolved in the BSA solution, and the hydrogels were prepared using the protocol described above, at a volume of 50 µL each. BSA-laden hydrogels were incubated in a 96-well plate filled with 200 µL PBS. At each time point, the supernatant was collected and 200 µL of fresh PBS were added back to the wells. The BSA concentrations in the hydrogel precursor solution (PEG monomers and BSA) and in the collected supernatant were measured with the Bio-Rad Protein Assay according to the manufacturer's instructions. The amount of BSA protein released from the hydrogels at each time point was calculated by measuring the concentration in the collected supernatant and multiplying that amount by the total volume. Cumulative release was determined by summing the total amounts released over time. The total BSA loaded into each hydrogel was calculated by multiplying the concentration in the hydrogel precursor solution by the volume of each gel (50 µL). The fraction of released BSA was calculated by dividing the cumulative release by the initial loading amount.

To characterize bFGF release, bFGF was added to the BSA-containing PEG monomer solution described above at a concentration of 2.5 µg mL^{-1}. Hdrogels were prepared at a volume of 50 µL each and incubated in a 96-well plate filled with 200 µL PBS. The supernatant was collected at predetermined time points and 200 µL of fresh PBS were added back to the wells. The concentration of bFGF in the collected supernatant was measured via enzyme-linked immunosorbent assay (PeproTech Human FGF-basic Standard ELISA Development Kit) according to the manufacturer's instructions.

5.8. Cell Proliferation

Human adult adipose-derived stem cells (ADSCs) were isolated from excised human adipose tissue with informed consent as previously described.[35] ADSCs were expanded for 4 passages in high glucose DMEM supplemented with 5 ng mL^{-1} basic fibroblast growth factor (bFGF), 100 U mL^{-1} penicillin, and 0.1 mg mL^{-1} streptomycin. hADSCs (passage 4) were used to monitor the biofunctionality of bFGF released from our PEG hydrogels. hADSCs were cultured in a 96-well plate (3000 cells/well) one day before the sample solution was added. After removing the old medium, 100 µL of bFGF-containing solution collected from the hydrogels

(or control solution) were added to the well, as were 100 μL of cell culture medium composed of high-glucose Dulbecco's Modified Eagle's Medium (Gibco), 10% fetal bovine serum (Gibco), and 100 U mL^{-1} penicillin/streptomycin (Gibco). PBS was used as a negative control, and fresh bFGF solution (10 ng mL^{-1}) in PBS was used as a positive control. Cells were cultured at 37 °C and 5% CO_2 for 72 h. Cell proliferation was measured with the CellTiter 96$^{®}$ AQueous One Solution Cell Proliferation Assay (Promega) according to the manufacturer's instructions.

5.9. Statistics

All experiments were performed in quadruplicate. Data are presented as mean ± standard deviation. Statistical analysis was performed using one-way analysis of variance with Tukey's correction for multiple comparisons ($\alpha = 0.05$) to compare all groups. The threshold for significance was set at $p < 0.05$.

[1] a) T. P. Richardson, M. C. Peters, A. B. Ennett, D. J. Mooney, *Nat. Biotechnol.* **2001**, *19*, 1029; b) R. Chen, D. Mooney, *Pharm. Res.* **2003**, *20*, 1103; c) Y. Tabata, *Tissue Eng.* **2003**, *9 Suppl. 1*, S5.
[2] a) J. Babensee, L. McIntire, A. Mikos, *Pharm. Res.* **2000**, *17*, 497; b) P. Tayalia, D. J. Mooney, *Adv. Mater.* **2009**, *21*, 3269; c) T. N. Vo, F. K. Kasper, A. G. Mikos, *Adv. Drug Delivery Rev.* **2012**, *64*, 1292.
[3] a) G. Schultz, W. Clark, D. S. Rotatori, *J. Cell. Biochem.* **1991**, *45*, 346; b) T. Mustoe, G. Pierce, A. Thomason, P. Gramates, M. Sporn, T. Deuel, *Science* **1987**, *237*, 1333.
[4] E. A. Wang, V. Rosen, J. S. D'Alessandro, M. Bauduy, P. Cordes, T. Harada, D. I. Israel, R. M. Hewick, K. M. Kerns, P. LaPan, *Proc. National Acad. Sci.* **1990**, *87*, 2220.
[5] a) M. J. Cross, L. Claesson-Welsh, *Trends Pharmacol. Sci.* **2001**, *22*, 201; b) H. P. Gerber, T. H. Vu, A. M. Ryan, J. Kowalski, Z. Werb, N. Ferrara, *Nat. Med.* **1999**, *5*, 623.
[6] R. R. Chen, E. A. Silva, W. W. Yuen, A. A. Brock, C. Fischbach, A. S. Lin, R. E. Guldberg, D. J. Mooney, *The FASEB Journal* **2007**, *21*, 3896.
[7] a) K. S. Anseth, A. T. Metters, S. J. Bryant, P. J. Martens, J. H. Elisseeff, C. N. Bowman, *J. Controlled Release* **2002**, *78*, 199; b) S. P. Zustiak, J. B. Leach, *Biotechnol. Bioeng.* **2011**, *108*, 197; c) G. W. Ashley, J. Henise, R. Reid, D. V. Santi, *Proc. National Acad. Sci.* **2013**, *110*, 2318.
[8] C.-C. Lin, K. S. Anseth, *Pharm. Res.* **2009**, *26*, 631.
[9] a) J. H. Lee, J. Kopecek, J. D. Andrade, *J. Biomed. Mater. Res.* **1989**, *23*, 351; b) N. P. Desai, J. A. Hubbell, *J. Biomed. Mater. Res.* **1991**, *25*, 829.
[10] a) C. Yang, P. D. Mariner, J. N. Nahreini, K. S. Anseth, *J. Controlled Release* **2012**, *162*, 612; b) K. C. Koehler, D. L. Alge, K. S. Anseth, C. N. Bowman, *Biomaterials* **2013**, *34*, 4150; c) D. V. Santi, E. L. Schneider, R. Reid, L. Robinson, G. W. Ashley, *Proc. National Acad. Sci.* **2012**, *109*, 6211.
[11] M. J. Roberts, M. D. Bentley, J. M. Harris, *Adv. Drug Delivery Rev.* **2002**, *54*, 459.
[12] K. Yang, A. Basu, M. Wang, R. Chintala, M. C. Hsieh, S. Liu, J. Hua, Z. Zhang, J. Zhou, M. Li, H. Phyu, G. Petti, M. Mendez, H. Janjua, P. Peng, C. Longley, V. Borowski, M. Mehlig, D. Filpula, *Protein Eng.* **2003**, *16*, 761.
[13] S. Kubetzko, C. A. Sarkar, A. Plückthun, *Mol. Pharmacol.* **2005**, *68*, 1439.
[14] a) A. A. Aimetti, A. J. Machen, K. S. Anseth, *Biomaterials* **2009**, *30*, 6048; b) T. Bal, B. Kepsutlu, S. Kizilel, *J. Biomed. Mater. Res. A* **2014**, *102*, 487.
[15] a) S. Lin-Gibson, R. L. Jones, N. R. Washburn, F. Horkay, *Macromolecules* **2005**, *38*, 2897; b) D. J. Waters, K. Engberg, R. Parke-Houben, L. Hartmann, C. N. Ta, M. F. Toney, C. W. Frank, *Macromolecules* **2010**, *43*, 6861.
[16] L. M. Weber, C. G. Lopez, K. S. Anseth, *J. Biomed. Mater. Res. A* **2009**, *90A*, 720.
[17] D. L. Elbert, A. B. Pratt, M. P. Lutolf, S. Halstenberg, J. A. Hubbell, *J. Controlled Release* **2001**, *76*, 11.
[18] P. G. Squire, P. Moser, C. T. O'Konski, *Biochemistry* **1968**, *7*, 4261.
[19] a) A. Metters, J. Hubbell, *Biomacromolecules* **2005**, *6*, 290; b) Y. Akagi, T. Matsunaga, M. Shibayama, U.-i. Chung, T. Sakai, *Macromolecules* **2009**, *43*, 488.
[20] J. Wen, S. M. Anderson, J. Du, M. Yan, J. Wang, M. Shen, Y. Lu, T. Segura, *Adv. Mater.* **2011**, *23*, 4549.
[21] a) R. G. Schoenmakers, P. van de Wetering, D. L. Elbert, J. A. Hubbell, *J. Controlled Release* **2004**, *95*, 291; b) S. P. Zustiak, J. B. Leach, *Biomacromolecules* **2010**, *11*, 1348.
[22] a) J. B. Leach, C. E. Schmidt, *Biomaterials* **2005**, *26*, 125; b) L. M. Weber, C. G. Lopez, K. S. Anseth, *J. Biomed. Mater. Res. Part A* **2009**, *90A*, 720.
[23] a) D. B. Pike, S. Cai, K. R. Pomraning, M. A. Firpo, R. J. Fisher, X. Z. Shu, G. D. Prestwich, R. A. Peattie, *Biomaterials* **2006**, *27*, 5242; b) C. C. Lin, K. S. Anseth, *Adv. Funct. Mater.* **2009**, *19*, 2325.
[24] B. D. Fairbanks, M. P. Schwartz, A. E. Halevi, C. R. Nuttelman, C. N. Bowman, K. S. Anseth, *Adv. Mater.* **2009**, 21.
[25] J. D. McCall, K. S. Anseth, *Biomacromolecules* **2012**, *13*, 2410.
[26] A. E. Eriksson, L. S. Cousens, L. H. Weaver, B. W. Matthews, *Proc. National Acad. Sci.* **1991**, *88*, 3441.
[27] D. S. W. Benoit, K. S. Anseth, *Acta Biomater.* **2005**, *1*, 461.
[28] M. A. Cole, K. C. Jankousky, C. N. Bowman, *Polym. Chem.* **2013**, *4*, 1167.
[29] A. M. Kloxin, A. M. Kasko, C. N. Salinas, K. S. Anseth, *Science* **2009**, *324*, 59.
[30] B. D. Fairbanks, M. P. Schwartz, C. N. Bowman, K. S. Anseth, *Biomaterials* **2009**, *30*, 6702.
[31] S. B. Anderson, C.-C. Lin, D. V. Kuntzler, K. S. Anseth, *Biomaterials* **2011**, *32*, 3564.
[32] A. Eliassi, H. Modarress, G. A. Mansoori, *J. Chem. Eng. Data* **1998**, *43*, 719.
[33] T. Canal, N. A. Peppas, *J. Biomed. Mater. Res.* **1989**, *23*, 1183.
[34] E. W. Merrill, K. A. Dennison, C. Sung, *Biomaterials* **1993**, *14*, 1117.
[35] J. H. Lai, G. Kajiyama, R. L. Smith, W. Maloney, F. Yang, *Sci. Rep.* **2013**, *3*, 3553.